IEEE Access
Multidisciplinary | Rapid Review | Open Access Journal

Received December 17, 2020, accepted December 31, 2020, date of publication January 6, 2021, date of current version January 13, 2021.

Digital Object Identifier 10.1109/ACCESS.2021.3049568

Joint Planning of Distributed PV Stations and EV Charging Stations in the Distribution Systems Based on Chance-Constrained Programming

XINSONG ZHANG, YANGYANG XU, SHENGNAN LU, CHENG LU, AND YUNXIANG GUO
College of Electrical Engineering, Nantong University, Nantong 226019, China

Corresponding author: Yunxiang Guo (guoyx@ntu.edu.cn)

This work was supported in part by the National Natural Science Foundation of China under Grant 61673226 and Grant 51877112, in part by the Natural Science Foundation of the Jiangsu Higher Education Institutions of China under Grant 17KJA470006, Grant 18KJA470003, and Grant 20KJD470004; and in part by the Nantong Basic Science Research Program under Grant JC2019125 and Grant JC2019127.

ABSTRACT Simultaneous deployment of the electric vehicle charging stations (EVCSs) and distributed photovoltaic stations (DPVSs) in the distribution systems is an effective way to reduce greenhouse gas emissions, promote renewable power adoption, and achieve sustainable development in energy utilization. In this context, how to deploy the EVCSs and DPVSs in the distribution systems with a reasonable scheme is of great importance. In this article, a joint planning model is developed to optimize locations and capacities of the EVCSs and DPVSs simultaneously to reduce energy losses in the distribution systems. In the joint planning model, constraints on bus voltage deviations and line currents are both formulated as chance constraints to ensure that the distribution systems are in reasonable operating statues. To quantify these two chance constraints, a scenario-based method is developed to calculate the probabilistic power flow of the distribution systems during a typical planning day, in which random characters of the DPVS generations and the EVCS charging loads are both considered. The joint planning model of the EVCSs and DPVSs developed in this article is difficult to be solved by mathematical optimization methods. Therefore, genetic algorithm (GA) is customized and utilized to solve the joint planning model of the EVCSs and DPVSs. Finally, a case study based on IEEE 33-bus distribution systems validates the joint planning model and its solving algorithm.

INDEX TERMS Electric vehicle charging station, distributed photovoltaic station, joint planning, genetic algorithm, chance constraints.

I. INTRODUCTION

Simultaneous development of renewable power generation and electric vehicle (EV) is an effective policy to reduce EVs' well-to-wheels greenhouse gas emissions, promote renewable power adoption, and achieve sustainable development in energy utilization, which attracts a great deal of attentions all around the world. At present, photovoltaic (PV) power stations are mainly integrated into the distribution systems as a form of distributed PV station (DPVS). It is obvious that large scale integrations of the DPVSs have dramatic impacts on the distribution systems [1], [2]. Meanwhile, EVs are mainly recharged from the distribution systems at the EV charging stations (EVCSs). In this context, the EVCSs become emerging electric loads and consequently have significant impacts on the distribution systems [3]–[5].

With incessant emerging of the DPVSs and EVCSs in the distribution systems, how to deploy the DPVSs and/or EVCSs with a suitable way becomes more and more important. Unreasonable constructing schemes of the DPVSs and/or EVCSs will deteriorate operating status of the distribution systems, for example, increasing energy losses, causing overloads of the distribution lines and transformers and leading to oversized bus voltage deviations [3], [4], [6], [7]. In this context, optimal planning of the DPVSs and/or EVCSs becomes a research hotspot in the area of the distribution systems planning.

With increasing penetration level of the DPVSs in the distribution systems, the impacts of the DPVSs on the distribution systems become increasingly prominent.

The associate editor coordinating the review of this manuscript and approving it for publication was Md. Rabiul Islam.

Therefore, optimal plan of the DPVSs in the distributions attracts a great deal of attentions from researchers. In [1], the locations of the DPVSs are optimized based on typical daily production/consummation curves of the DPVSs/loads, aiming to minimize active and reactive power losses. Reference [8] proposes an optimization methodology to identify proper locations and sizes of the DPVSs in the distribution systems, which can be solved by the particle swarm optimization technique. In [9], an optimization is built to optimize locations and sizes of the DPVSs to be connected to the distribution systems. Main contribution of [9] is to adopt self-organizing hierarchical binary particle swarm algorithm to solve the optimization, which can achieve more excellent performance than other algorithms. In [10], the flower pollination algorithm is utilized to determine optimal locations and capacities of the DPVSs, with a purpose of reducing energy losses in distribution systems. In [11], an analytical approach is developed to determine sizes and locations of the DPVSs in the distribution systems, in which energy loss reductions, voltage profile improvements and economic benefits are considered simultaneously. Reference [12] develops an integrated GIS and robust optimization framework to determine locations and sizes, where the DPVSs should be built so that the penetration level of the DPVSs within a given region can be maximized.

With the popularity of EVs in traffic systems, the impacts of the EVCS charging loads on the distribution systems become more and more prominent because EVs are mainly recharged at the EVCSs. In this context, how to determine optimal locations and capacities of the EVCSs in the distribution systems attracts more and more attentions from scholars and engineers all over the world. [5] develops a stepwise framework to determine optimal locations and capacities of the EVCSs in the distribution systems, in which operating constraints and stability of the distribution systems are considered simultaneously. In [13], a hybrid algorithm based on genetic algorithm (GA) and improved version of conventional particle swarm optimization is designed to find optimal placement of the EVCSs in the distribution systems in Allahabad, India. The optimization objective in [13] is to improve voltage profile and quality in the Allahabad distribution systems. In [14], an optimization is proposed to optimize the EVCS allocation schemes for a target of minimizing the annualized social cost of whole EV charging systems, which can be transformed into a type of mixed integer second-order cone programming and be efficiently solved by appropriate mathematical methods. The mainly contribution of [14] is to consider multi-types of charging facilities during the planning stage. With the consideration of uncertain charging demands, a bi-level optimization is developed in [15] to address the planning issues of the EVCSs with a purpose of minimizing the investments and operations cost of the EVCSs. The bi-level optimization can be reformulated into a single-level mixed integer second-order cone programming, which can be easily solved by appropriate mathematical methods. In [16], the interactions between the distribution companies (DISCO) and the EVCS owners are analyzed based on Nash bargaining theory. Based on this, a mixed integer nonlinear programming is utilized to determine the optimal place and size of the EVCSs and the price of energy transacted between the DISCO and the EVCS owners so as to maximizing profits of the DISCO and the EVCS owners. In consideration of the development of charging demand, [17] establishes a siting and sizing optimization for the electric taxi EVCSs that selects the optimal constructing plan of charging stations from candidate construction plans for achieving the lowest social costs.

Up to now, a lot of research has been done on the planning of the DPVSs or EVCSs in the distribution systems. In the distribution systems, the DPVSs and EVCSs jointly have impacts on the operating status. Therefore, it is a reasonable way to execute a joint planning of the DPVSs and EVCSs in the distribution systems. However, there are few researches in this area. In [18], an optimization is developed to joint deploy the DPVSs and EVCSs in the distribution systems with a cost-effective way from the perspective of a social planner. In the optimization developed in [18], the EV charging load is modeled as a spatially dispatchable electric load because the EV owners are assumed to make their charging decisions depending on the guidance from navigation systems. A comprehensive model is developed in [19] for jointly sitting and sizing of the DPVSs, the EVCSs and the energy storage systems in the distribution systems, in which, time-varying nature of the DPVS generations and EV charging loads are considered simultaneously. Reference [20] proposes a multidisciplinary approach to investigate optimal sites and sizes of the DPVSs and EVCSs on a coupled transportation and distribution systems. Main contributions of [20] is to consider explicit constraints on EV driving range and probabilistic constraints on quality of charging service.

For each EV to be charged, charging power, charging start time and initial charging state of charge (SOC) are all stochastic. Consequently, charging loads of the EVCS have obvious random characteristics. In addition, generations of the DPVS also have obvious random characteristics, which come from primary energy. These two random characteristics should be elaborately considered in joint planning of the DPVSs and EVCSs in the distribution systems, however, they are not sufficiently considered in [18]–[20].

In this article, a planning model is developed to execute joint planning of the EVCSs and DPVSs based on the power flow analysis for the distribution systems, i.e., optimize locations and capacities of the EVCSs and DPVSs simultaneously to reduce energy losses in the distribution systems. The joint planning model of the EVCSs and DPVSs developed in this article is difficult to be solved by mathematical optimization methods, therefore, GA is utilized to solve it. Finally, a case study based on the IEEE 33-bus distribution systems validate the joint planning model and its solving algorithm.

Main contributions of this article are detailed as below:

1) Random characteristics of the EVCS changing loads and the DPVS generations are not sufficiently considered in existing works, such as [18]–[20]. To bridge this gap, a scenario-based method is developed to calculate the probabilistic power flow of the distribution systems with considerations of random DPVS generations and EVCS charging loads, and the constructing scheme of the DPVSs and EVCSs is optimized based on the probabilistic power flow calculation results.

2) To ensure that the distribution systems operate in a reasonable operating statue, constraints on bus voltage deviations and line currents are both formulated as chance constraints in the planning model based on the probabilistic power flow calculation results.

3) GA is customized and utilized to solve the joint planning model of the EVCSs and DPVSs effectively. More concretely, crossover and mutation operators in GA are specially designed according to characters of the joint planning model.

II. EVCSs' CHARGING LOAD SIMULATION AND PROBABILISTIC POWER FLOW CALCULATION OF THE DISTRIBUTION SYSTEMS

The DPVSs and EVCSs both have significant impacts on the distribution systems. So, planners should select locations and sizes of the DPVSs and EVCSs simultaneously based on investigating operating statues of the distribution systems. The EVCS charging loads are stochastic because charging power, charging start time and initial charging SOC of each EV charged in the EVCS are all stochastic. Meanwhile, the DPVS generations are also stochastic, which come from primary energy. Under this condition, the distribution systems operate in a random manner rather than a deterministic manner with large-scale integrations of the DPVSs and EVCSs. In this context, it is difficult to describe the operating statues of the distribution systems accurately based on deterministic power flow results. In contrast, the operating statues of the distribution systems must be described based on probabilistic power flow results. In this article, a scenario-based method is utilized to calculate the probabilistic power flow of the distribution systems during the typical planning day. Establishing the scenario probability model of the random variable is the basis to execute probabilistic power flow analysis by means of the scenario-based method. This article intends to establish two scenario probability models that can reflect stochastic characters of the EVCS charging loads and DPVS generations respectively by clustering daily charging load curve set of the EVCSs and daily output power curve set of the DPVSs by means of the K-means clustering (KMC) [21]–[23].

A. SIMULATION OF EVCS CHARGING LOADS

Currently, it is difficult to construct the scenario probability model of the EVCS charging loads only based on historical data because of the lack of field measurement data. Therefore, Monte Carlo simulation (MCS) technology is utilized to simulate daily charging loads of the EVCSs to provide sufficient data for constructing the scenario probability model. Several random factors considered in the MCS include charging start time, initial charging SOC, charging mode and charging duration, which are detailed as follows:

1) CHARGING POWER

At present, the charging pile can provide two charging modes for EV drivers to choose, i.e., fast charging mode and slow charging mode. The charging mode is selected randomly by EV drivers and the charging power of a single EV is supposed to be constant and determined by the charging mode selected by EV drivers. In this context, the charging power of a single EV, denoted here by P_{ch} is subject to a Bernoulli distribution, which is shown as follows:

$$\begin{cases} \mathrm{P_r}\{P_{\mathrm{ch}} = P_{\mathrm{cha,q}}\} = p \\ \mathrm{P_r}\{P_{\mathrm{ch}} = P_{\mathrm{cha,n}}\} = 1 - p \quad 0 < p < 1 \end{cases} \tag{1}$$

where $\mathrm{P_r}\{.\}$ represents the probability of the event expressed in $\{\}$. $P_{\mathrm{cha,q}}$ and $P_{\mathrm{cha,n}}$ denotes the charging power of a single EV in fast and slow charging modes respectively. p is the probability of an event that the EV driver chooses the fast charging mode to recharge his EV battery. In this article, p is supposed to be jointly determined by charging start time and initial charging SOC.

2) INITIAL CHARGING SOC

It is assumed that the EV driver will pull into the EVCSs for charging immediately after his last trip during a day. Under this condition, the initial charging SOC of the EV battery is determined by EV's daily driving mileage and can be estimated by:

$$E_0 = (1 - \frac{d}{L_{\max}}) \times 100\% \tag{2}$$

where E_0 is the initial charging SOC of the EV battery. d is a random variable representing EV's daily driving mileage, which is affected by traffic behaviors of the EV drivers. $L_{\max}$ is an endurance mileage of the fully charged EV. In this article, probability distribution characteristics of the variable d is described by a Lognormal distribution, which is shown as follows:

$$f_d(x) = \frac{1}{d\sqrt{2\pi}\sigma_{\mathrm{d}}} \exp[-\frac{(\ln d - u_{\mathrm{d}})^2}{2\sigma_{\mathrm{d}}^2}] \tag{3}$$

where μ_{d} and σ_{d} are 3.09 and 0.16 respectively.

3) CHARGING START TIME

It is assumed that the EV driver will pull into the EVCSs for charging immediately after his last trip during a day. Under this assumption, the ending time of the last trip is just the charging start time of the EV to be charged, denoted here as T_{sc}. The probability distribution character of the charging start time can be described by probability density function

illustrated as (4).

$$f_{T_{\mathrm{sc}}}(x)=\begin{cases}\dfrac{1}{\sigma_{\mathrm{sc}}\sqrt{2\pi}}\exp[-\dfrac{(x-\mu_{\mathrm{sc}})^2}{2\sigma_{\mathrm{sc}}^2}],\\ (\mu_{\mathrm{sc}}-12)<x\le 24\\ \dfrac{1}{\sigma_{\mathrm{sc}}\sqrt{2\pi}}\exp[-\dfrac{(x+24-\mu_{\mathrm{sc}})^2}{2\sigma_{\mathrm{sc}}^2}],\\ 0<x\le(\mu_{\mathrm{sc}}-12)\end{cases} \tag{4}$$

where μ_{sc} and σ_{sc} are 17.6 and 3.4 respectively.

4) CHARGING DURATION

The charging duration of the EV, denoted here as T_{c} can be calculated as

$$T_{\mathrm{c}}=\frac{(1-E_0)C_{\mathrm{b}}}{P_{\mathrm{ch}}\eta} \tag{5}$$

where C_{b} denotes capacity of the EV battery and η denotes charging efficiency of the EV battery. It can be found from (5) that the EV is supposed to be charged to fully charging state when calculating charging duration of the EV. That is to say, the charging/discharging limits are implicitly considered in the model. In (5), both initial charging SOC and charging power are random variables, so the charging duration of the EV is also a random variable.

With considerations of random factors described above, MCS is utilized to simulate daily charging load of an EVCS equipped with m charging piles. In the MCS, a simulating day is equally divided into T simulation periods and the length of each simulation period is T_{step}. The simulation steps are detailed as follows:

Step 1: Index of simulation count, denoted here as n_{sim} and charging power in each simulation period, denoted here as $P_{\mathrm{cha},t}$ are both initialized to be zero, i.e., let $n_{\mathrm{sim}}=0$ and $P_{\mathrm{cha},t}=0$, $1\le t\le T$.

Step 2: Let $n_{\mathrm{sim}}=n_{\mathrm{sim}}+1$ and start a new round of simulation. The number of available charging piles in each simulation period, denoted here as $m_{\mathrm{pile},t}$ is initialized to be m, that is, let $m_{\mathrm{pile},t}=m$, $1\le t\le T$. When an EV pulls into the EVCS for charging, the EVCS cannot provide charging service for it if there is just no vacant charging pile at that time. In the MCS, a parameter denoted here as m_{tag} is designed to represent the number of failed recharging attempts during the day resulted from no vacant charging pile in the EVCS. The parameter m_{tag} is initialized to be m, that is $m_{\mathrm{tag}}=0$.

Step 3: Randomly generate a set of EV to be charged, denoted here as Ω_{ev}. Each EV in set Ω_{ev} can be characterized by three random variables: charging start time, initial charging SOC and charging power. Three random variables are generated as follows. Firstly, randomly generate a charging start time of the EV that obeys the probability distribution character illustrated in (4). Secondly, randomly generate a daily mileage of the EV, which follows the probability distribution character illustrated in (3), and then calculate initial charging SOC of the EV according to (2). Thirdly, randomly generate a random number ς that obey a uniform distribution between [0, 1]. If $\varsigma\le p$, EV drivers select the fast charging mode to recharge his EV, i.e., let $P_{\mathrm{ch}}=P_{\mathrm{cha,q}}$, otherwise, let $P_{\mathrm{ch}}=P_{\mathrm{cha,n}}$.

Step 4: Sort all EVs in set Ω_{ev} by their charging start time. Let $m_{\mathrm{ev}}=0$, which indexes the EV in set Ω_{ev}.

Step 5: Let $m_{\mathrm{ev}}=m_{\mathrm{ev}}+1$ and calculate the charging duration of the $m_{\mathrm{ev}}^{\mathrm{th}}$ EV in set Ω_{ev} according to (5). And then, calculate the first- and last- simulation periods when charging the $m_{\mathrm{ev}}^{\mathrm{th}}$ EV according to (6) and (7), which are respectively denoted as t_1 and t_2.

$$t_1=\frac{T_{\mathrm{sc}}\times 60}{T_{\mathrm{step}}}+1 \tag{6}$$

$$t_2=\frac{(T_{\mathrm{sc}}+T_{\mathrm{c}})\times 60}{T_{\mathrm{step}}}+1 \tag{7}$$

Step 6: If there are available charging pile(s) at all simulation periods from simulation periods t_1 to t_2, i.e., $m_{\mathrm{pile},t}>0$ ($\forall t\in[t_1,t_2]$), the EVCS can provide charging service for the $m_{\mathrm{ev}}^{\mathrm{th}}$ EV. Under this condition, update charging power and available number of the charging piles according to (8) and (9), and then go back to Step 5 and continue.

$$P_{\mathrm{cha},t}=P_{\mathrm{cha},t}+\frac{P_{\mathrm{ch}}}{n_{\max}},\quad t_1\le t\le t_2 \tag{8}$$

$$m_{\mathrm{pile},t}=m_{\mathrm{pile},t}-1,\quad t_1\le t\le t_2 \tag{9}$$

If there is no vacant charging pile at one or more simulation periods from simulation periods t_1 to t_2, the EVCS cannot provide charging service for $m_{\mathrm{ev}}^{\mathrm{th}}$ EV. Under this condition, update m_{tag} as:

$$m_{\mathrm{tag}}=m_{\mathrm{tag}}+1 \tag{10}$$

If m_{tag} reaches a predetermined threshold, denoted here as $m_{\mathrm{tag,m}}$, finish present simulation and record daily charging power curve pertaining to this simulation. Otherwise, go back to Step 5 and continue.

Step 7: If the simulation count n_{sim} reaches maximum simulation count of the MCS, denoted here as $n_{\max}$, stop the simulation. In this case, a set of daily EVCS charging loads which contain $n_{\max}$ daily charging power curves can be obtained. Otherwise, go back to Step 2 and start a new round of simulation.

In the MCS, parameter $m_{\mathrm{tag,m}}$, is relevant to the average number of the EVs entering the EVCS for charging during the day. Therefore, it can be determined according to daily average number of the EVs charged in a similar EVCS.

B. CONSTRUCTION OF THE SCENARIO PROBABILITY MODEL FOR EVCS CHARGING LOADS

To build a scenario probability model for EVCS charging loads, $n_{\max}$ daily charging load curves given by the MCS are clustered by the KMC. If the number of clusters is set to be $n_{\mathrm{c,ev}}$, $n_{\max}$ charging load curves can be divided into $n_{\mathrm{c,ev}}$ clusters according to the similarity of the charging load curves, as illustrated in Fig.1. Each cluster center can be seemed as a scenario in the scenario probability

model for EVCS charging loads. The ratio of the number of charging load curves in a cluster and the number of the total charging load curves is defined as the scenario probability.

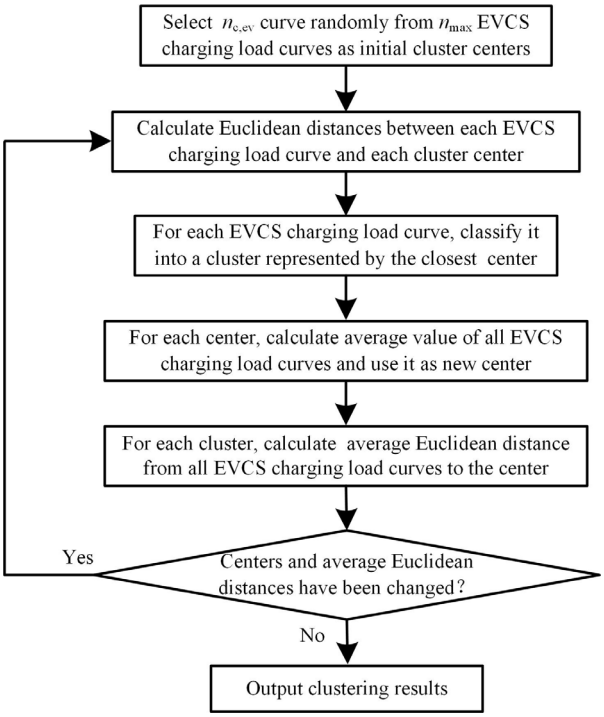

FIGURE 1. Flowchart of clustering EVCS charging load curves by the K-means clustering method.

C. CONSTRUCTION OF THE SCENARIO PROBABILITY MODEL FOR DPVS GENERATIONS

At present, a large number of DPVSs are connected to the distribution systems, most of which are equipped with Supervisory Control and Data Acquisition (SCADA) systems. In this context, a mass of historical output power data of the DPVSs are available. The KMC is also utilized to cluster historical output power data of the DPVSs to build a scenario probability model for output power of the DPVSs, which includes $n_{c,pv}$ scenarios. Here, $n_{c,pv}$ is a predetermined number of clusters when clustering historical output power data of the DPVSs.

D. PROBABILISTIC POWER FLOW CALCULATION OF DISTRIBUTION SYSTEMS

The fluctuations of the DPVS generations and the EVCS charging loads are assumed to be independent each other. Under this assumption, a probability scenario model is generated for calculating probabilistic power flow of the distribution systems during the typical day, which is composed of $n_{c,ev} \times n_{c,pv}$ scenarios. The probabilistic power flow of the distribution systems during the typical day are obtained by gathering power flow results in all scenarios according to the probability of each scenario.

III. JOINT PLANNING MODEL OF THE EVCSS AND DPVSS BASED ON CHANCE-CONSTRAINED PROGRAMMING

The DPVSs and EVCSs are both new components appearing on the distribution systems simultaneously, and have significant impacts on the operating status of the distribution systems. Therefore, it is necessary to execute joint planning of the EVCSs and DPVSs, i.e., to determine optimal locations and capacities of the EVCSs and DPVSs in the distribution systems. The random characters of the EVCS charging loads and DPVS generations must be elaborately considered in the joint planning model. In this article, the random factors described above are considered by a means of chance-constrained programming. Chance-constrained programming belongs to stochastic programming, and it has been successfully applied in the field of power systems research [24]–[27]. In the chance-constrained programming, bus voltages and line currents can exceed the predetermined ranges but the probabilities are less than a predetermined level (i.e., a confidence level). Excessive voltage deviations and line currents can easily be adjusted to reasonable ranges in operations, if they only appear occasionally. Therefore, Chance-constrained programming is suitable for the joint planning of the EVCSs and DPVSs in the distribution systems and is expected to give a reasonable planning result.

A. OPTIMIZATION OBJECTIVE

Large scale integrations of the DPVSs and EVCSs have significant impacts on the distribution systems, including changing energy loss of the distribution systems. As a result, to minimize the energy loss of the distribution system in the typical planning day is formulated as an optimization objective of the joint planning model of the DPVSs and EVCSs as follows:

$$\min F_{\text{loss}} = \sum_{t=1}^{T_f} \sum_{l \in \Omega_{\text{br}}} E(\Delta P_{\text{loss},l,t}) \frac{24}{T_f} \tag{11}$$

where F_{loss} is an expected energy loss of the distribution system during the typical planning day. When calculating probabilistic power plow of the distribution systems, the typical planning day is divided equally into T_f time periods, and t indices the time periods. l is an index of the distribution line, Ω_{br} is a set of the distribution lines, $\Delta P_{\text{loss},l,t}$ is a random variable, which represents the energy loss of distribution line l in time period t. The probabilistic distribution characteristic of $\Delta P_{\text{loss},l,t}$ is relevant to constructing scheme of the DPVSs and EVCSs, which can be obtained through calculating probabilistic power flow of the distribution systems. $E(\cdot)$ is an operator for calculating expectations of the random variables given in ().

In this article, capacities and locations of the DPVSs and EVCSs are optimizes based on probabilistic analysis of the distribution systems during a typical planning day. In this context, planning results depends on which typical planning day is selected to some extent. If planners want to obtain

better planning results, they should extend the planning horizon from one day to a month, even to several years [28].

B. CONSTRAINTS

1) CONSTRAINT ON NUMBER OF THE EVCSS

$$\sum_{i=1}^{N_{\mathrm{ch}}} x_i = M_{\mathrm{ch}} \tag{12}$$

where M_{ch} is a total number of the EVCSs to be constructed in the planning area, which can be predetermined by planners according to total number of the EVs together with municipal planning. N_{ch} is a total number of candidate locations selected for constructing the EVCSs in the planning area, and i indexes the candidate locations. x_i is a binary optimization variable of the joint planning model of the DPVSs and EVCSs, representing whether or not an EVCS is constructed at candidate location i. If x_i equals to '1', an EVCS is constructed at candidate location i, otherwise no EVCS is constructed at candidate location i.

2) CONSTRAINT ON NUMBER OF THE DPVSS

$$\sum_{j=1}^{N_{\mathrm{pv}}} y_j = M_{\mathrm{pv}} \tag{13}$$

where M_{pv} is a total number of the DPVSs to be constructed in the planning area, depending on current situation of the distribution systems together with municipal planning. N_{pv} is a total number of candidate buses that are available for the DPVSs in the distribution systems, and j indexes the candidate buses. y_j is also a binary optimization variable of the joint planning model of the DPVSs and EVCSs, representing whether or not a DPVS is connected to candidate bus j. For y_j, '1' means a DPVS is to candidate bus j, while '0' means no EVCS is connected to candidate bus j.

3) CONSTRAINT ON TOTAL CAPACITY OF THE EVCSS

$$\sum_{i=1}^{N_{\mathrm{ch}}} x_i z_i = C_{\mathrm{ch}} \tag{14}$$

where z_i is a capacity of the EVCS constructed at candidate location i. In this article, the EVCSs to be constructed in the planning area are divided into Q_{ev} categories by their capacities. In this context, z_i is a discrete optimization variable in the joint planning model of the DPVSs and EVCSs. C_{ch} is total capacity of the EVCSs constructed in the planning area, which can be predetermined by multi factors, such as total number of the EVs, total investments of the EVCSs, construction cost of a single charging pile and municipal planning.

4) CONSTRAINT ON TOTAL CAPACITY OF THE DPVSS

$$\sum_{j=1}^{N_{\mathrm{pv}}} y_j w_j = C_{\mathrm{pv}} \tag{15}$$

where w_j is a capacity of the DPVS connected to candidate bus j. In this article, the DPVSs to be connected to the distribution systems are divided into Q_{pv} categories by their capacities. In this context, w_j is a discrete optimization variable in the joint planning model of the DPVSs and EVCSs. C_{pv} is total capacity of the DPVSs to be connected to the distribution systems, which are mutually predetermined according to total investment of the DPVSs, construction cost of the DPVSs and municipal planning.

5) CHANCE CONSTRAINT ON BUS VOLTAGE DEVIATIONS

$$P_r\left\{\frac{U_k - U_{\mathrm{N}}}{U_{\mathrm{N}}} \times 100\% > \alpha\%\right\} \le \beta_1 \quad k \in \Omega_{\mathrm{bus}} \tag{16}$$

where k indexes the buses in the distribution systems, and Ω_{bus} is a set of the distribution buses. U_k is a voltage of bus k, which is a random variable and related to constructing scheme of the DPVSs and EVCSs. $\alpha\%$ is a percentage, representing maximum allowable deviation of the bus voltage, β_1 is a predetermined confidence level.

6) CHANCE CONSTRAINT ON LINE CURRENTS

$$P_r\left\{I_l > I_{l,\max}\right\} \le \beta_2 \quad l \in \Omega_{\mathrm{br}} \tag{17}$$

where l indexes the lines in the distribution systems and Ω_{br} is a set of the distribution lines. I_l is a random variable indicating the current in distribution line l. The probability characteristics of the currents in distribution lines are related to the constructing scheme of the DPVSs and EVCSs. $I_{l,\max}$ is a maximum allowable current in distribution line l. β_2 is a predetermined confidence level.

The constraint on power balance in the distribution systems is considered in calculating power flow by means of the probability scenario model. Therefore, it is not illustrated directly in the panning model.

IV. SOLUTION OF THE JOINT PLANNING MODEL OF THE EVCSs AND DPVSs

The joint planning model of the EVCSs and DPVSs mentioned above is an optimization with chance constraints, which incorporates binary optimization variables and discrete optimization variables. In addition, the probabilistic power flow calculation model in the joint planning model of the EVCSs and DPVSs is nonlinear. So, it is difficult to solve the joint planning model of the EVCSs and DPVSs by a mathematical optimization method. GA is a typical evolutionary algorithm and has strong adaptability and global optimization capabilities. It has been successfully employed to solve many optimization problems in the field of the power systems, such as unit commitment, reactive power optimization, and transmission network expansion planning [29]–[31]. The characteristics of the joint planning model of the EVCSs and DPVSs are similar to those of unit commitment, reactive power optimization, and transmission network expansion planning. So, GA is also utilized to solve the joint planning model of the EVCSs and DPVSs.

A. CODING AND POPULATION INITIALIZATIO

In this article, an integer coding scheme is utilized to encode a feasible solution of the joint planning model of the EVCSs and DPVSs into a chromosome, as illustrated in Fig. 2.

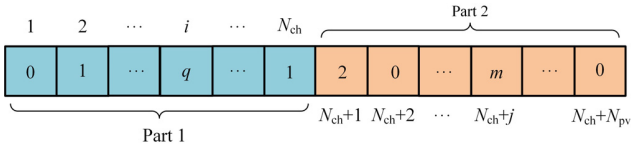

FIGURE 2. Scheme of chromosome coding.

The chromosome consists of $(N_{ch}+N_{pv})$ coding points and can be divided into two independent parts. The first part is from the first coding point to N_{ch}^{th} coding point, representing the constructing scheme of the EVCSs. If i^{th} coding point of the chromosome equals to '0', it means that no EVCS is constructed at candidate location i $(i = 1, 2, 3, \cdots, N_{ch})$. In contrast, if i^{th} coding point equals to 'q', an EVCS belonging to q^{th} category is constructed at candidate location i, and its capacity is $C_{ev,q}$ $(q = 1, 2, 3, \cdots, Q_{ev})$. Remaining coding points in the chromosome belong to the second part, which represents the constructing scheme of the DPVSs. If $(N_{ch}+j)^{th}$ coding point equals to '0', there is no DPVS connected to candidate bus j $(j = 1, 2, 3, \cdots, N_{pv})$. In contrast, if $(N_{ch}+j)^{th}$ coding point equals to 'm', a DPVS belonging to m^{th} category is connected to candidate bus j, and its capacity is $C_{pv,\,m}$ $(m = 1, 2, 3, \cdots, Q_{pv})$.

To satisfy the constraint on number of the EVCSs, it must be ensured that only M_{ch} coding points in the first part of the chromosome equal to non-zero integers. In addition, only M_{pv} coding points in the second part of the chromosome are ensured to be non-zero integers for satisfying the constraint on number of the DPVSs. To ensure that each chromosome in initial population fulfills the above requirements, the chromosome is generated as follows.

Step1: Let all code points of the chromosome to be '0'.

Step2: Select M_{ch} coding points randomly from the first part of the chromosome and change their values from '0' to a random integer that is equal to or less than Q_{ev}.

Step3: Select M_{pv} coding points randomly from the second part of the chromosome and change their values from '0' to a random integer that is equal to or less than Q_{pv}.

B. FITNESS CALCULATION

The kernel of GA is to evaluate each chromosome in the population by means of fitness calculations [29]–[31]. The calculations of chromosome fitness are detailed as follow:

Step1: Decode the chromosome to be evaluated for determining constructing locations/buses and capacities of all EVCSs and DPVSs. Calculate total capacities of all EVCSs and DPVSs to be constructed, respectively denoted here as C_{t-ev} and C_{t-pv}.

Step2: Based on the constructing scheme of the EVCSs and DPVSs determined in Step 1, calculate probabilistic power flow of the distribution systems during the planning day by means of the scenario-based method.

Step 3: Deal with the constraints given by (14)-(17) by means of penalty function method and calculate fitness of the chromosome by (18).

$$V_{fit} = F_{max}/F_{loss} - \eta_1 \times V_{p1} - \eta_2 \times V_{p2} - \eta_3 \times V_{p3} - \eta_4 \times V_{p4} \tag{18}$$

where V_{fit} denotes fitness of the chromosome to be evaluated. F_{max} is a large positive number given in advance to guarantee V_{fit} is always not negative. η_1, η_2, η_3 and η_4 are predetermined penalty coefficients. V_{p1}, V_{p2}, V_{p3} and V_{p4} respectively quantify a violation degree of the constraints given by (14)-(17), which can be calculated by (19)-(22). It can be found from (18) that the better the chromosome to be evaluated, the greater the fitness.

$$V_{p1} = |C_{ch} - C_{t-ev}| \tag{19}$$

$$V_{p2} = |C_{pv} - C_{t-pv}| \tag{20}$$

$$V_{p3} = \sum_{k \in \Omega_{bus}} \max\left[P_r\left\{\frac{|U_k - U_N|}{U_N} \times 100\% > \alpha\%\right\} - \beta_1, 0\right] \tag{21}$$

$$V_{p4} = \sum_{l \in \Omega_{br}} \max\left[P_r\{I_l > I_{l,max}\} - \beta_2, 0\right] \tag{22}$$

C. GENETIC OPERATORS

In this article, mutation operator and crossover operator are customized according to characters of the joint planning model of the EVCSs and DPVSs for enhancing performance of the GA. They are detailed as below.

1) CROSSOVER OPERATOR

To ensure that any chromosome after crossover operation satisfies the constraints given by (12) and (13), a specialized crossover operator is designed, as illustrated in Figure 3.

Figure 3 depicts that the customized crossover operator consists three crossover operations, which is detailed as follows:

Step 1: Randomly select two chromosomes to be crossed from the population.

Step 2: Exchange the coding string after N_{ch}^{th} code point of the two chromosomes with crossover probability P_c to complete the first crossover operation.

Step 3: Randomly generate candidate crossover position $N_{can1}(1 < N_{can1} < N_{ch})$ until obtaining a feasible crossover position N_{cr1}. The criteria for judging whether candidate crossover position N_{can1} is a feasible crossover position is as follows: from coding points $N_{can1}+1$ to N_{ch}, the numbers of coding points with no-zero value in the two chromosomes are consistent. Exchange the coding string from coding points $N_{cr1}+1$ to N_{ch} with crossover probability P_c to complete the second crossover operation.

Step 4: Randomly generate candidate crossover position $N_{can2}(N_{ch} < N_{can2} < N_{ch}+N_{pv})$ until a feasible crossover position N_{cr2} is obtained. The criteria for judging whether

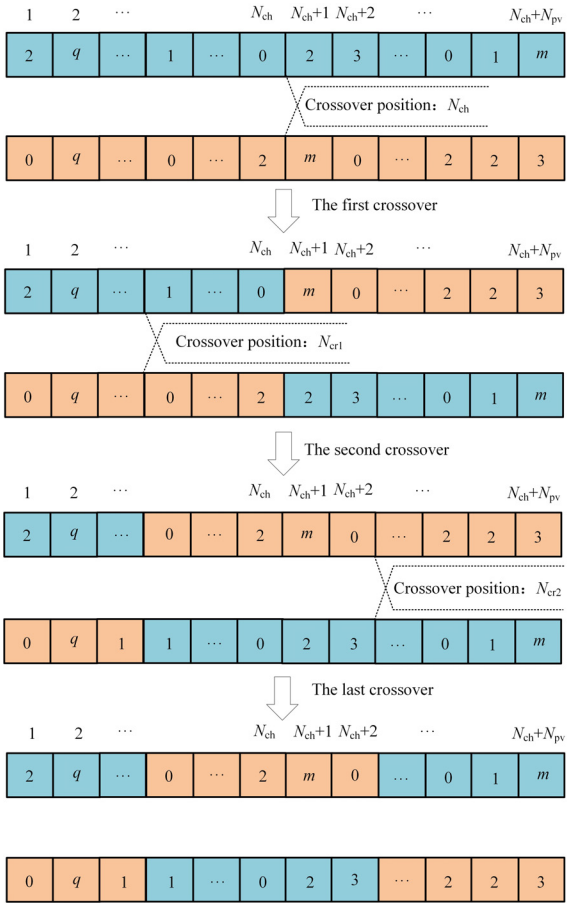

FIGURE 3. Customized crossover operator.

candidate crossover position N_{can2} is a feasible crossover position is as follows: after coding point N_{can2}, the numbers of coding points with no-zero value in the two chromosomes are consistent. Exchange the coding string after N_{cr2} with crossover probability P_c to complete the third crossover operation.

2) MUTATION OPERATOR

Mutation operator might cause the chromosome to violate the constraints given by (12) and (13). To avoid this situation, a specialized mutation operator is designed in this article, as illustrated in Figure 4.

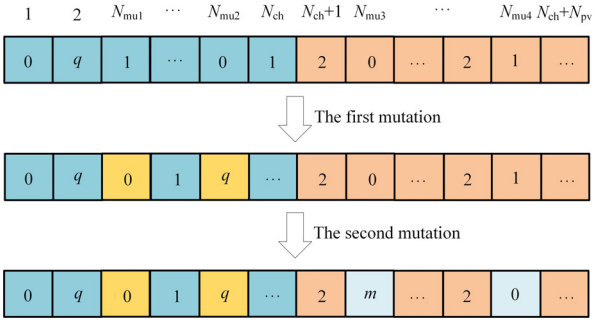

FIGURE 4. Customized mutation operator.

The customized mutation operator includes two mutation operations and is detailed as follows:

Step 1: Select a chromosome to be mutated from the population.

Step 2: Randomly select two coding points in the first part of the chromosome as mutation positions, entailed respectively as N_{mu1} and $N_{mu2}(1 \leq N_{mu1} \leq N_{ch}, 1 \leq N_{mu2} \leq N_{ch})$. It must be endured that one of the two mutation coding positions equals to '0', the other is a no-zero integer.

Step 3: Perform the first mutation operation at mutation coding positions N_{mu1} and N_{mu2} simultaneously with mutation operator probability P_m. If the value of the mutation position equals to '0', it is mutated to a random non-zero integer not greater than Q_{ev}, otherwise, it is mutated to '0'.

Step 4: Randomly select two coding points in the second part of the chromosome as mutation positions, entailed respectively as N_{mu3} and N_{mu4} ($N_{ch} \leq N_{mu3} \leq N_{ch} + N_{pv}$, $N_{ch} \leq N_{mu4} \leq N_{ch} + N_{pv}$). It must be endured that one of the two mutation coding positions equals to '0', the other is a no-zero integer.

Step 5: Perform the second mutation operation at mutation coding positions N_{mu3} and N_{mu4} simultaneously with mutation operator probability P_m. If the value of the mutation position equals to '0', it is mutated to a random non-zero integer not greater than Q_{pv}, otherwise, it is mutated to '0'.

D. FLOWCHART OF THE GA

The flowchart of the GA designed for solving the joint planning model of the EVCSs and DPVSs is illustrated as Figure 5. In Figure 5, when GA evolves to the maximum evolution time, entailed here as G_{max} it can be considered as convergent [29]–[31].

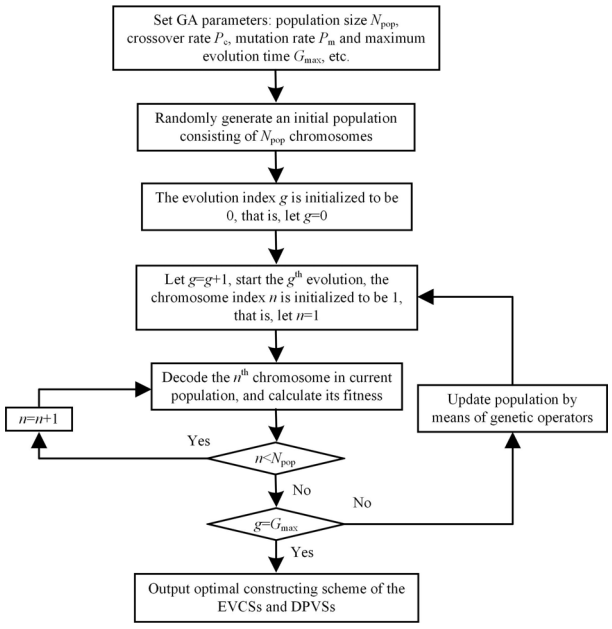

FIGURE 5. Flowchart of the GA customized for solving the joint planning model of the EVCSs and DPVSs.

V. CASE STUDY

In this section, the effectiveness of the proposed joint planning model and corresponding solving algorithm are validated through a detailed case study in the IEEE 33-bus distribution system.

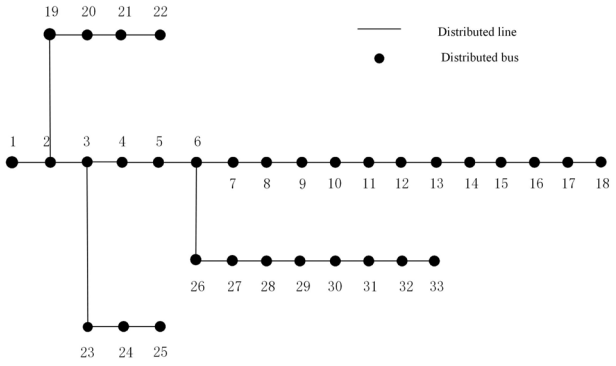

FIGURE 6. Topology of the IEEE 33-bus distribution system.

A. CASE INTRODUCTION

The IEEE 33-bus distribution system consists of 33 distribution lines and 32 distribution buses, as illustrated in Figure 6. The rated voltage of the IEEE 33-bus distribution system is 12.66 kV. The parameters of the distribution lines and reference loads in distribution buses can be found in [32], which are not included here. For calculating probabilistic power plow of the IEEE 33-bus distribution system, a typical planning day is divided into 24 time periods, i.e., variable T_{f} in (11) is set to be 24. The active power curve during the typical planning day is shown in p.u. in Figure 7. In addition, it is assumed that the power factor of loads in each bus remains unchanged during the typical planning day. Maximum allowable currents of all distribution lines in the IEEE 33-bus distribution system are illustrated in Table 1, which are obtained by raising 10% from currents under the reference loads.

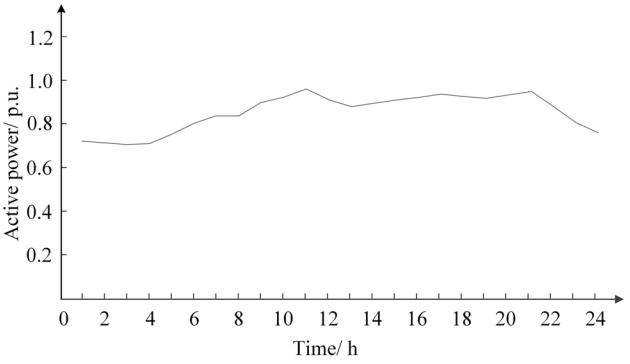

FIGURE 7. The active power curve during the typical planning day (p.u.).

In the case study, it's assumed that the total numbers of the EVCSs and DPVSs to be constructed in the IEEE 33-bus distribution system are both 4, i.e., $M_{\mathrm{ch}} = 4$, and $M_{\mathrm{pv}} = 4$. In the case study, the EVCSs and DPVSs are all divided into 6 categories according to their capacities, i.e., $Q_{\mathrm{ev}} = 6$, and $Q_{\mathrm{pv}} = 6$. The capacities of the EVCSs belonging to 6 categories are respectively 2 MW, 4MW, 6 MW, 8 MW, 10 MW, 12 MW and 14 MW, and the capacities of the DPVSs belonging to 6 categories are respectively 1.6 MW, 3.2 MW, 4.8MW, 6.4 MW, 8.0 MW, and 9.6 MW. To satisfy the charging requirements in the planning area, total capacity of EVCSs to be constructed is set to be 20 MW, i.e., $C_{\mathrm{ev}} = 20$ MW. Total capacity of DPVSs to be constructed is set to be 16 MW, i.e., $C_{\mathrm{pv}} = 16$ MW. Maximum allowable voltage deviation percentage is set to be 10%, i.e., $\alpha\%$=10%. Two predetermined confidence levels with respect to bus voltage deviations and line currents are both set to be 0.05, i.e., $\beta_1 = 0.05$, and $\beta_2 = 0.05$.

TABLE 1. Maximum available currents of the distribution lines.

No.	$I_{l,\max}$ (A)	No.	$I_{l,\max}$ (A)	No.	$I_{l,\max}$ (A)	No.	$I_{l,\max}$ (A)
1	230.10	9	34.6	17	4.94	25	68.01
2	203.96	10	31.26	18	19.84	26	64.9
3	144.72	11	28.05	19	14.88	27	61.78
4	136.44	12	25.04	20	9.89	28	58.4
5	132.16	13	21.44	21	4.94	29	51.45
6	60.82	14	14.33	22	52.17	30	23.66
7	49.41	15	11.30	23	47.05	31	15.27
8	37.97	16	8.12	24	23.41	32	3.62

Some parameters on the GA customized for solving the joint planning model of the EVCSs and DPVSs are as follows: the population size is 50, the maximum evolution time is 200, crossover probability and mutation probability are respectively set to be 0.2 and 0.08. In (18), $F_{\max}$ is set to be 5000, penalty coefficients η_1, η_2, η_3 and η_4 are respectively set to be 0.6, 0.02, 0.03 and 0.05.

B. SCENARIO PROBABILITY MODELS OF THE EVCS CHARGING LOADS AND DPVS GENERATIONS

Daily charging load of a typical EVCS equipped with 50 charging piles is simulated by the MCS for providing data to construct the scenario probability model of the EVCS charging loads. Each charging pile installed in the typical EVCS can operate on fast or slow charging mode depending on choices of the EV drivers. The charging power of the two modes is respectively 20 kW and 5 kW. Some parameters in the MCS are as follows: the capacity of the EV battery is 40 kW·h, i.e., $C_{\mathrm{b}} = 40$ kW·h; the charging efficiency is 0.95, i.e., $\eta = 0.95$; the endurance mileage of the fully charged EV is 200 km, i.e., $L_{\max} = 200$ km; and maximum simulation count of the MCS is 10000, i.e., $n_{\max} = 10000$. The probability of the event that the EV driver chooses fast

charging mode is set as: if $E_0 > 0.7, p = 0.0$, if $E_0 \leq 0.7$ and $T_{sc} \leq 12, p = 0.2$, and if $E_0 \leq 0.7$ and $T_{sc} > 12, p = 0.5$. The parameter $m_{tag,m}$ can be determined according to the average number of the EVs to be charged in similar EVCS, which is set to be 50 in the case.

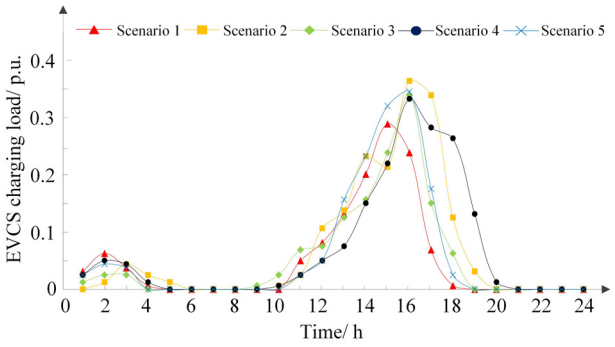

FIGURE 8. Scenario probability model of the EVCS charging loads (p.u.).

10000 daily EVCS charging load curves provided by the MCS are clustered by the KMC to establish the scenario probability model of the EVCS charging loads, as illustrated in Figure 8. The scenario probability model of the EVCS charging loads consists of 5 typical charging load curves, and probabilities with respect to them are respectively 0.228, 0.195, 0.204, 0.164 and 0.209. In Figure 8, the charging power is expressed in p.u., and the reference value is calculated according to the charging power in fast charging mode and the number of charging piles, that is $50 \times 20 = 1000$ kW.

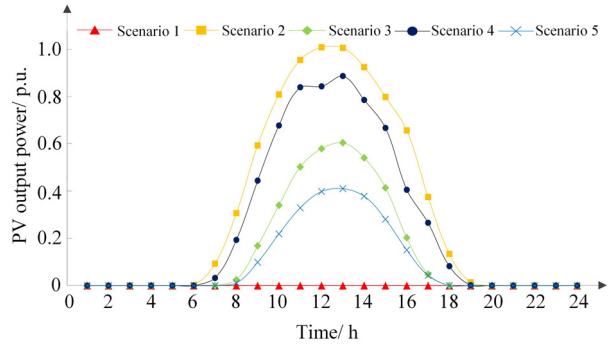

FIGURE 9. Scenario probability model of the DPVS generations (p.u.).

Field measurement data from a DPVS in Suzhou, China are clustered by the KMC to establish the scenario probability model of the DPVS generations, as illustrated in Figure 9. The scenario probability model of the DPVS generations consists of 5 typical generation curves, and probabilities with respect to them are respectively 0.257, 0.151, 0.203, 0.189 and 0.2. In Fig.9, the output power of the DPVS is expressed in p.u., and the reference value is installed capacity of the DPVS.

C. SOLVING PERFORMANCES ON THE CUSTOMIZED GA

In this article, GA is customized and utilized to solve the joint planning model of the EVCSs and DPVSs. More concretely,

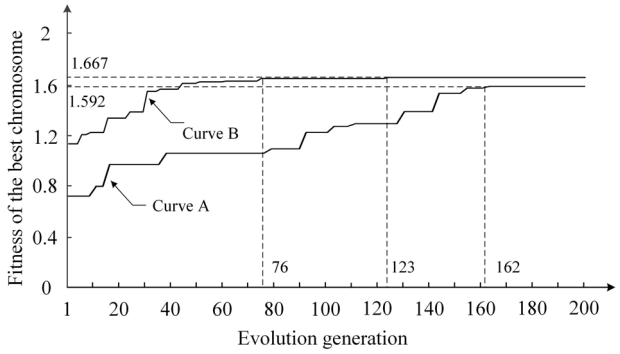

FIGURE 10. The performance on solution of general GA and the customized GA.

crossover and mutation operators in GA are specially designed according to characters of the joint planning model to be solved for improving solution performance. Solution performance on the customized GA is illustrated as Curve B in Figure 10, which depicts fitness of the best chromosome in each generation. It can be found from the Curve B that fitness of the best chromosome in each generation increases significantly as the population evolves, especially before the 40th generation. After the 40th generation, the fitness upgradation becomes slower than ever before. The customized GA tends to convergence after 76th generation, and converges to final solution in the 123rd generation. The program of the customized GA runs on ThinkPad T470 personal laptop (Intel(R) Core (TM) i5-7200U CPU@2.50 GHz + RAM 8.00 GB) and the computational time for convergence is 72 seconds.

For comparison, general GA is also employed to solve the joint planning model of the EVCSs and DPVSs without any modification for the optimization to be solved. The program of general GA also runs on ThinkPad T470 personal laptop (Intel(R) Core (TM) i5-7200U CPU@2.50 GHz + RAM 8.00 GB). Under this condition, fitness of the best chromosome in each generation is illustrated as Curve A in Figure 10. From Curves A and B, it can be found that the performance on solution of general GA is significantly poorer than that of the customized GA. Firstly, the general GA takes 93 seconds to converge to final solution in the 162nd generation, while the customized GA only takes 72 seconds to reach final solution in the 123rd generation. Secondly, the general GA converges to a local optimal solution, whose fitness is 1.592. In contrast, the customized GA can obtain a better solution, whose fitness is 1.667. As can be seen from the description above, the customized GA can solve the joint planning model of the EVCSs and DPVSs effectively.

D. RESULTS AND ANALYSIS

The joint planning scheme of the EVCSs and DPVSs given by the customized GA is illustrated in Figure 11. Figure 11 depicts that four EVCSs with capacities of 8 MW, 4 MW, 2 MW, and 6 MW are respectively constructed at Buses 1, 2, 3 and 4, meanwhile four DPVSs with capacities

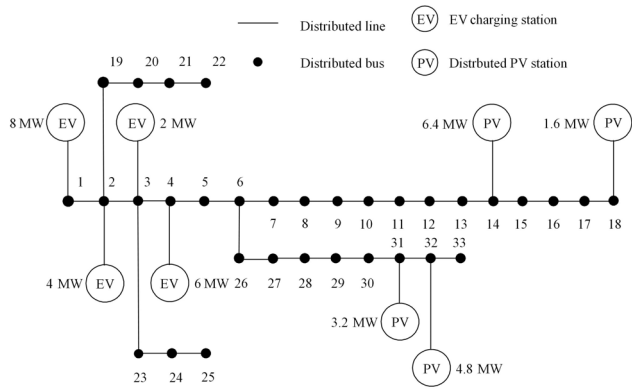

FIGURE 11. Joint planning scheme of the EVCSs and DPVSs.

of 6.4MW, 1.6 MW, 3.2 MW and 4.8 MW are respectively connected to Buses 14, 18, 31 and 32. In this context, expected energy loss of the distribution system during the typical planning day is 2999.14 kW·h. In addition, bus voltage deviations or line currents does not exceed the prescribed limits during the typical day, that is to say, the IEEE 33-bus distribution system operates very well during the typical planning day. The EVCSs and DPVSs are usually constructed at geographically adjacent buses, even at the same bus to improve operating status of the distribution systems, especially to reduce the energy lose. However, the EVCSs and DPVSs are not constructed at geographically adjacent buses in the case study, because temporal characteristics of the EVCS charging loads and the DPVS generations are significantly different each other.

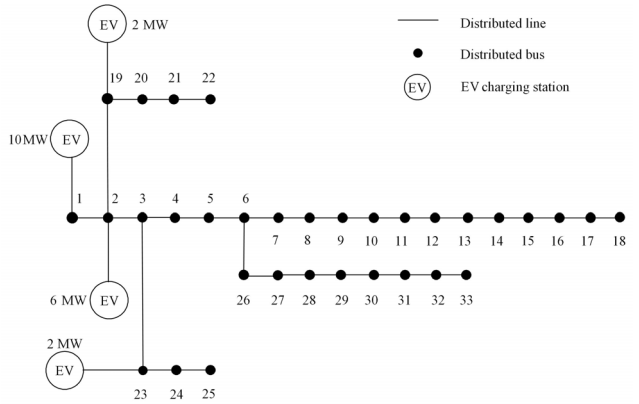

FIGURE 12. Constructing scheme of the EVCSs given in the first stage.

The methodology proposed in this article executes a joint plan of the EVCSs and DPVSs, giving the constructing scheme of the EVCSs and DPVSs simultaneously. For comparison, plan of the EVCSs and DPVSs is divided into two stages that can be executed in sequence. In the first stage, constructing scheme of the EVCSs is optimized and illustrated in Figure 12. In this context, both locations and capacities of the EVCSs are different with those in joint planning scheme of the EVCSs and DPVSs. More concretely, four EVCSs with capacities of 10 MW, 6 MW, 2 MW, and 2 MW are respectively constructed at Buses 1, 2, 19 and 23. From constructing scheme of the EVCSs illustrated in Figure 12, constructing scheme of the DPVSs is optimized in the second stage, which is illustrated in Figure 13. Under this condition, both locations and capacities of the DPVSs are also change, i.e., four DPVSs with capacities of 1.6MW, 1.6 MW, 3.2 MW and 9.6 MW respectively are connected to Buses 14, 15, 17 and 31.

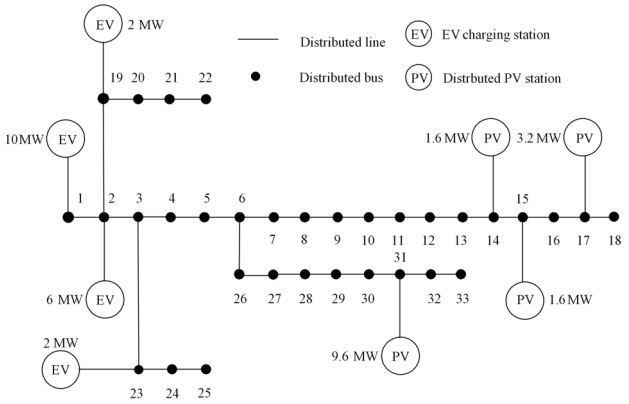

FIGURE 13. Constructing scheme of the EVCSs and DPVSs with two-stage optimization.

When the EVCSs and DPVSs are constructed in the IEEE 33-bus distribution system as the scheme given in two-stage optimization, expected energy loss of the distribution system during the typical planning day increases from 2999.14 kW·h to 3056.72 kW·h. Meanwhile, currents at Lines 16, 18 and 30 are possibly over the prescribed limits during the typical day, but the probabilities are all less than predetermined confidence level (i.e. be less than 0.05), which are illustrated in Figure 14. In a word, operating statue of the IEEE 33-bus distribution system is getting worse under this condition. From the comparisons above, it can be concluded that the joint planning methodology developed in this article can achieve more excellent constructing scheme of the EVCSs and DPVSs.

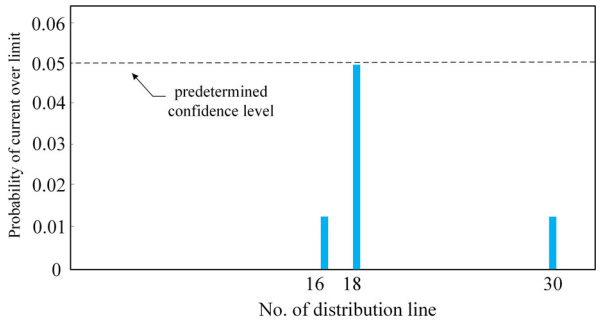

FIGURE 14. Probabilities of current over limit when the EVCSs and DPVSs are constructed as the scheme given in two-stage optimization.

In joint planning of the EVCSs and DPVSs, the confidence levels with respect to bus voltage deviations and line currents are predetermined by the planners. In fact, the confidence

levels might have impacts on the joint planning scheme of the EVCSs and DPVSs. To investigate these impacts, we also execute joint planning of the EVCSs and DPVSs under different confidence levels. When parameters β_1 and β_2 decrease from 0.05 to 0.0, the joint planning scheme of the EVCSs and DPVSs is illustrated in Figure 15, and expected energy loss of the distribution system during the typical planning day increases from 2999.14 kW·h to 3009.8 kW·h. When parameters β_1 and β_2 increase from 0.05 to 0.1, the joint planning scheme of the EVCSs and DPVSs is illustrated in Figure 16, and expected energy loss of the distribution system during the typical planning day decreases from 2999.14 kW·h to 2985.96 kW·h.

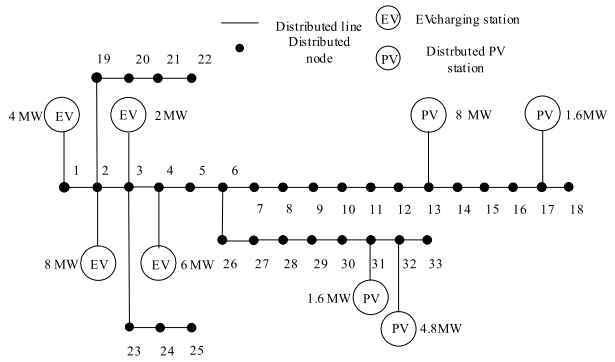

FIGURE 15. Joint planning scheme of the EVCSs and DPVSs when parameters β_1 and β_2 are set to be 0.0.

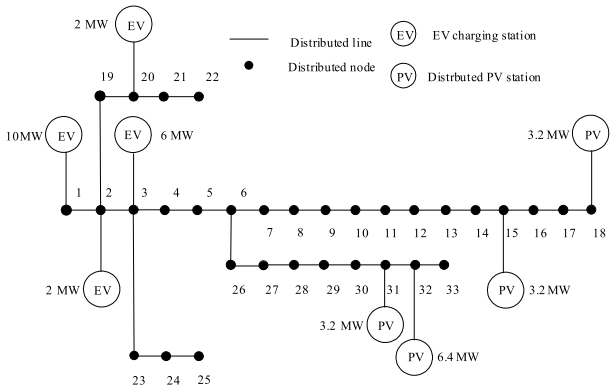

FIGURE 16. Joint planning scheme of the EVCSs and DPVSs when parameters β_1 and β_2 are set to be 0.1.

From Figures 11, 15 and 16, it can be found that the confidence levels have significant impacts on the joint planning scheme of the EVCSs and DPVSs. Locations and capacities of some EVCSs and DPVSs change as the confidence levels change. For example, if the confidence levels increase from 0.05 to 0.1, the DPVS originally connected to Bus 14 is connected to Bus 15, meanwhile the capacity decreases from 6.4 MW to 3.2 MW. In addition, the higher the confidence levels are, the lower expected energy loss of the distribution system during the typical planning day is. The planners should select the confidence levels carefully according to their risk preferences and actual situations of the distribution systems.

VI. CONCLUSION

In this article, a chance-constrained joint planning mode is built to jointly optimize locations and capacities of the EVCSs and DPVSs to be constructed in the distribution systems. The optimization objective is to reduce energy losses in the distribution systems under a premise of ensuring that the distribution systems operate in a reasonable way. GA is customized and utilized to solve the joint planning model of the EVCSs and DPVSs.

In this article, a case study based on the IEEE 33-bus distribution system is executed to validate the joint planning model and its solving algorithm. In future work, we will execute more case studies, especially some case studies on actual/larger distribution systems to improve the joint planning model and its solving algorithm.

In addition, the planning horizon is defined as a typical planning day in this article. In future work, we will extend it from a day to several years and consider growths of loads and the EVCS charging loads during the extended planning horizon.

REFERENCES

[1] R. Prenc, D. Skrlec, and V. Komen, "Optimal PV system placement in a distribution network on the basis of daily power consumption and production fluctuation," in *Proc. Eurocon*, Jul. 2013, pp. 777–783.

[2] M. E. Khodayar, M. R. Feizi, and A. Vafamehr, "Solar photovoltaic generation: Benefits and operation challenges in distribution networks," *Electr. J.*, vol. 32, no. 4, pp. 50–57, May 2019.

[3] C. Crozier, T. Morstyn, and M. McCulloch, "The opportunity for smart charging to mitigate the impact of electric vehicles on transmission and distribution systems," *Appl. Energy*, vol. 268, Jun. 2020, Art. no. 114973.

[4] H. R. Galiveeti, A. K. Goswami, and N. B. D. Choudhury, "Impact of plug-in electric vehicles and distributed generation on reliability of distribution systems," *Eng. Sci. Technol., Int. J.*, vol. 21, no. 1, pp. 50–59, Feb. 2018.

[5] T. Kunj and K. Pal, "Optimal location planning of EV charging station in existing distribution network with stability condition," in *Proc. 7th Int. Conf. Signal Process. Integr. Netw. (SPIN)*, Feb. 2020, pp. 1060–1065.

[6] S. Seme, N. Lukač, B. Štumberger, and M. Hadžiselimović, "Power quality experimental analysis of grid-connected photovoltaic systems in urban distribution networks," *Energy*, vol. 139, pp. 1261–1266, Nov. 2017.

[7] E. N. M. Silva, A. B. Rodrigues, and M. D. G. D. Silva, "Stochastic assessment of the impact of photovoltaic distributed generation on the power quality indices of distribution networks," *Electr. Power Syst. Res.*, vol. 135, pp. 59–67, Jun. 2016.

[8] S. Bhuyan, M. Das, and K. C. Bhuyan, "Particle swarm optimizations based DG allocation in local PV distribution networks for voltage profile improvement," in *Proc. Int. Conf. Comput., Electr. Commun. Eng. (ICCECE)*, Dec. 2017, pp. 1–4.

[9] N. Phuangpornpitak and S. Tia, "Optimal photovoltaic placement by self-organizing hierarchical binary particle swarm optimization in distribution systems," *Energy Procedia*, vol. 89, pp. 69–77, Jun. 2016.

[10] T. Prasetyo, S. Sarjiya, and L. M. Putranto, "Optimal sizing and siting of PV-based distributed generation for losses minimization of distribution using flower pollination algorithm," in *Proc. Int. Conf. Inf. Commun. Technol. (ICOIACT)*, Jul. 2019, pp. 779–783.

[11] M. Jamil and A. S. Anees, "Optimal sizing and location of SPV (solar photovoltaic) based MLDG (multiple location distributed generator) in distribution system for loss reduction, voltage profile improvement with economical benefits," *Energy*, vol. 103, pp. 231–239, May 2016.

[12] B. Pillot, N. Al-Kurdi, C. Gervet, and L. Linguet, "An integrated GIS and robust optimization framework for solar PV plant planning scenarios at utility scale," *Appl. Energy*, vol. 260, Feb. 2020, Art. no. 114257.

[13] A. Awasthi, K. Venkitusamy, S. Padmanaban, R. Selvamuthukumaran, F. Blaabjerg, and A. K. Singh, "Optimal planning of electric vehicle charging station at the distribution system using hybrid optimization algorithm," *Energy*, vol. 133, pp. 70–78, Aug. 2017.

[14] L. Luo, W. Gu, S. Zhou, H. Huang, S. Gao, J. Han, Z. Wu, and X. Dou, "Optimal planning of electric vehicle charging stations comprising multi-types of charging facilities," *Appl. Energy*, vol. 226, pp. 1087–1099, Sep. 2018.
[15] B. Zhou, G. Chen, Q. Song, and Z. Y. Dong, "Robust chance-constrained programming approach for the planning of fast-charging stations in electrified transportation networks," *Appl. Energy*, vol. 262, Mar. 2020, Art. no. 114480.
[16] A. Pahlavanhoseini and M. S. Sepasian, "Optimal planning of PEV fast charging stations using Nash bargaining theory," *J. Energy Storage*, vol. 25, Oct. 2019, Art. no. 100831.
[17] X. Meng, W. Zhang, Y. Bao, Y. Yan, R. Yuan, Z. Chen, and J. Li, "Sequential construction planning of electric taxi charging stations considering the development of charging demand," *J. Cleaner Prod.*, vol. 259, Jun. 2020, Art. no. 120794.
[18] L. Luo, W. Gu, Z. Wu, and S. Zhou, "Joint planning of distributed generation and electric vehicle charging stations considering real-time charging navigation," *Appl. Energy*, vol. 242, pp. 1274–1284, May 2019.
[19] O. Erdinc, A. Tascikaraoglu, N. G. Paterakis, I. Dursun, M. C. Sinim, and J. P. S. Catalao, "Comprehensive optimization model for sizing and siting of DG units, EV charging stations, and energy storage systems," *IEEE Trans. Smart Grid*, vol. 9, no. 4, pp. 3871–3882, Jul. 2018.
[20] H. Zhang, S. J. Moura, Z. Hu, W. Qi, and Y. Song, "Joint PEV charging network and distributed PV generation planning based on accelerated generalized benders decomposition," *IEEE Trans. Transport. Electrific.*, vol. 4, no. 3, pp. 789–803, Sep. 2018.
[21] Y. Hong and S. Kwong, "Learning assignment order of instances for the constrained K-means clustering algorithm," *IEEE Trans. Syst., Man, Cybern. B. Cybern.*, vol. 39, no. 2, pp. 568–574, Apr. 2009.
[22] J. Cao, Z. Wu, J. Wu, and H. Xiong, "SAIL: Summation-based incremental learning for information-theoretic text clustering," *IEEE Trans. Cybern.*, vol. 43, no. 2, pp. 570–584, Apr. 2013.
[23] X. Huang, Y. Ye, and H. Zhang, "Extensions of kmeans-type algorithms: A new clustering framework by integrating intracluster compactness and intercluster separation," *IEEE Trans. Neural Netw. Learn. Syst.*, vol. 25, no. 8, pp. 1433–1446, Aug. 2014.
[24] A. Stuhlmacher and J. L. Mathieu, "Water distribution networks as flexible loads: A chance-constrained programming approach," *Electr. Power Syst. Res.*, vol. 188, Nov. 2020, Art. no. 106570.
[25] F. Qi, M. Shahidehpour, Z. Y. Li, F. S. Wen, and C. Z. Shao, "A chance-constrained decentralized operation of multi-area integrated electricity–natural gas systems with variable wind and solar energy," *IEEE Trans. Sustain. Energy*, vol. 11, no. 4, pp. 2230–2240, Oct. 2020.
[26] M. Hemmati, B. Mohammadi-Ivatloo, M. Abapour, and A. Anvari-Moghaddam, "Optimal chance-constrained scheduling of reconfigurable microgrids considering islanding operation constraints," *IEEE Syst. J.*, vol. 14, no. 4, pp. 5340–5349, Dec. 2020.
[27] B. Odetayo, M. Kazemi, J. MacCormack, W. D. Rosehart, H. Zareipour, and A. R. Seifi, "A chance constrained programming approach to the integrated planning of electric power generation, natural gas network and storage," *IEEE Trans. Power Syst.*, vol. 33, no. 6, pp. 6883–6893, Nov. 2018.
[28] X. Zhang, M. Shahidehpour, A. Alabdulwahab, and A. Abusorrah, "Optimal expansion planning of energy hub with multiple energy infrastructures," *IEEE Trans. Smart Grid*, vol. 6, no. 5, pp. 2302–2311, Sep. 2015.
[29] H.-T. Yang, P.-C. Yang, and C.-L. Huang, "A parallel genetic algorithm approach to solving the unit commitment problem: Implementation on the transputer networks," *IEEE Trans. Power Syst.*, vol. 12, no. 2, pp. 661–668, May 1997.
[30] A. Ozdemir, J. Y. Lim, and C. Singh, "Post-outage reactive power flow calculations by genetic algorithms: Constrained optimization approach," *IEEE Trans. Power Syst.*, vol. 20, no. 3, pp. 1266–1272, Aug. 2005.
[31] M. Guerrero, F. G. Montoya, R. Baños, A. Alcayde, and C. Gil, "Community detection in national-scale high voltage transmission networks using genetic algorithms," *Adv. Eng. Informat.*, vol. 38, pp. 232–241, Oct. 2018.
[32] B. Venkatesh, R. Ranjan, and H. B. Gooi, "Optimal reconfiguration of radial distribution systems to maximize loadability," *IEEE Trans. Power Syst.*, vol. 19, no. 1, pp. 260–266, Feb. 2004.

XINSONG ZHANG received the B.E. degree in electrical engineering from the Xi'an University of Technology, Xi'an, China, in 2002, the M.Sc. degree in electrical engineering from Xi'an Jiaotong University, Xi'an, in 2005, and the Ph.D. degree from Hohai University, Nanjing, China, in 2013. He joined the Faculty of Nantong University, China, in 2006. From 2018 to 2019, he was an Academic Visitor with the Department of Electronic and Electrical Engineering, University of Bath, Bath, U.K. He is currently an Associate Professor with the School of Electrical Engineering, Nantong University. His research interests include power systems operation and planning, wind power integration, and energy storage systems.

YANGYANG XU received the B.S. degree in electrical engineering from the Jincheng College, Nanjing University of Aeronautics and Astronautics, Nanjing, China, in 2018. He is currently pursuing the M.S. degree in control science and control engineering with Nantong University, Nantong, China. His research interests include power systems operation and planning, renewable energy control technology, and electric vehicle charging network planning.

SHENGNAN LU received the B.S. degree in automation from the Changzhou Institute of Technology, Changzhou, China, in 2017. She is currently pursuing the master's degree in control science and engineering with Nantong University, Nantong, China. Her research interests include power systems operation and planning and renewable energy generation technology.

CHENG LU received the B.S. and M.S. degrees in control engineering from Hohai University, Changzhou, China, in 2010 and 2013, respectively, and the Ph.D. degree in electrical engineering from Hohai University, Nanjing, China, in 2017. He is currently a Lecturer with the School of Electrical Engineering, Nantong University, Nantong, China. His research interests include sliding mode control, adaptive control, and neural networks.

YUNXIANG GUO received the B.S. degree in electrical engineering from North China Electric Power University, Baoding, China, in 2009, and the Ph.D. degree in high voltage and insulation technology from North China Electric Power University, Beijing, China, in 2017. He is currently a Lecturer with the School of Electrical Engineering, Nantong University, Nantong, China. His research interests include distribution systems operation, renewable energy control, and electric vehicle charging technology.